Design, Synthesis, and Pharmacological Profile of Novel Fused Pyrazolo[4,3-*d*]pyridine and Pyrazolo[3,4-*b*][1,8]naphthyridine Isosteres: A New Class of Potent and Selective Acetylcholinesterase Inhibitors

Eliezer J. Barreiro,*[,†,‡] Celso A. Camara,[‡] Hugo Verli,[†,‡] Leonora Brazil-Más,[§] Newton G. Castro,[§] Wagner M. Cintra,[§] Yasco Aracava,[§] Carlos R. Rodrigues,[†] and Carlos A. M. Fraga[†,‡]

Laboratório de Avaliação e Síntese de Substâncias Bioativas (LASSBio), Faculdade de Farmácia, Universidade Federal do Rio de Janeiro, C. P. 68.006, 21944-910, Rio de Janeiro, RJ, Brazil, Departamento de Química Orgânica, Instituto de Química, Universidade Federal do Rio de Janeiro, Rio de Janeiro, RJ, Brazil, and Departamento de Farmacologia Básica e Clínica, Instituto de Ciências Biomédicas, Centro de Ciências da Saúde, Universidade Federal do Rio de Janeiro, Rio de Janeiro, RJ, Brazil

Received September 10, 2002

A new family of tacrine (THA) analogues (**7**−**9**, **12**), containing the azaheterocyclic pyrazolo-[4,3-*d*]pyridine or pyrazolo[3,4-*b*][1,8]naphthyridine systems as isosteres of the quinoline ring of THA, has been synthesized. The compounds were tested in rat brain cholinesterases using Ellman's method, and all were fully efficacious in inhibiting the enzymes. Compounds **9** and **12b** were the most potent against acetylcholinesterase (AChE), showing IC_{50} of 6.0 and 6.4 μM, and were less active against rat brain butyrylcholinesterase, showing selectivity indexes of 5.3 and 20.9, respectively. Compounds **7**−**9** and **12** were also tested for their acute neurotoxicity in vitro, using cultured rat cortical cells. Compounds **7** and **8** were not significantly toxic; **9** was toxic at 500 μM, but not at 100 μM. The naphthyridine derivatives **12a** and **12b** showed a significant concentration-dependent neurotoxicity, being able to kill most cells at 500 μM. Molecular dynamic simulation using the X-ray crystal structure of AChE from *Torpedo californica* was used to explain the possible binding mode of these new THA isosteres.

Introduction

Alzheimer's disease (AD) is a neurodegenerative disorder characterized by a progressive impairment of cognitive function which seems to be associated with deposition of amyloid protein and neuronal loss, as well as with altered neurotransmission in the brain.[1] Much of the functional deficit in AD has been correlated with extensive morphological and functional derangement of the central cholinergic system. The efficacy of cholinergic therapies in this disease validates and supports the cholinergic hypothesis of AD.[2] Several strategies have been explored to enhance cholinergic transmission,[3] such as acetylcholinesterase (AChE) inhibitors[4] (e.g., galanthamine[5] (**1**)), acetylcholine (ACh) precursors[1] (e.g., choline, **2**), nicotinic agonists[6] (e.g., ABT-418, **3**), muscarinic agonists[7] (e.g., arecholine, **4**) or acetylcholine releasers[3] such as linopirdine (**5**). AChE inhibition has proven to be a successful strategy to ameliorate cholinergic deficit and to promote symptomatic improvement of AD patients.[8] Tacrine (9-amino-1,2,3,4-tetrahydroacridine, THA, **6**), described in 1953, was the first AChE inhibitor approved for the palliative treatment of AD senile dementia.[9] Its clinical usefulness is limited, however, owing to undesirable side effects, specially hepatotoxicity,[10,11] and current research is focused on developing new AChE inhibitors with improved activity and reduced adverse side effects.

In the scope of a research program aiming at the design, synthesis, and evaluation of new neuroactive lead-compound candidates with beneficial effects in treatment of AD as AChE inhibitors, we became interested in developing new THA analogues. The new compounds **7**−**9** described in this study were structurally planned with basis in the bioisosteric relationship between the quinoline ring, included in the 1,2,3,4-tetrahydroacridine system of THA, and the azaheterocyclic pyrazolo[3,4-*b*]pyridine system.[12] This new isosteric relationship was discovered in the study of the new antimalarial compound **10**, an analogue of mefloquine (**11**) (Figure 1).[12]

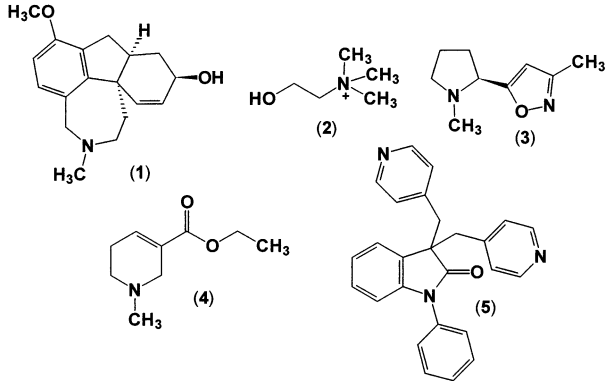

The new THA analogues **7**−**9** (Figure 1) are positional isomers, designed in order to investigate the eventual contribution of different *N*-phenyl orientations around the azaheterocyclic system in the AChE activity.

* To whom correspondence should be addressed. Fax/Phone: +55−21−25626644. E-mail: eliezer@ufrj.br. http://www.farmacia.ufrj.br/lassbio.

† LASSBio, Faculdade de Farmácia, Universidade Federal do Rio de Janeiro.

‡ Instituto de Química, Universidade Federal do Rio de Janeiro.

§ Instituto de Ciências Biomédicas, Universidade Federal do Rio de Janeiro.

10.1021/jm020391n CCC: $25.00
Published on Web 02/28/2003

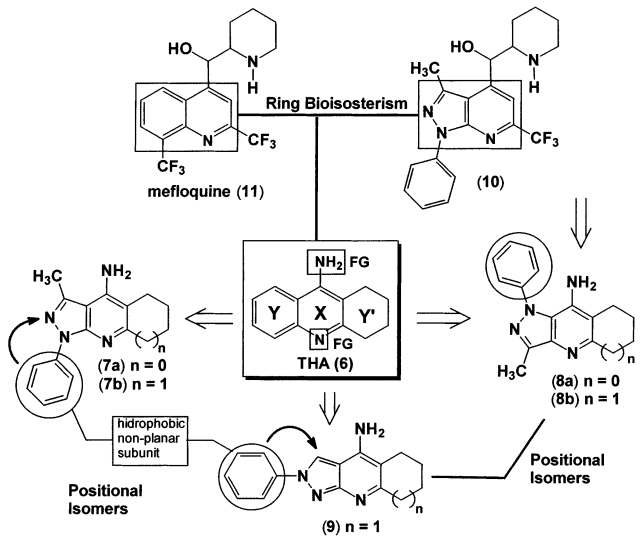

Figure 1. Design concept of new pyrazolopyridine THA analogues **7**−**9**.

The crystallographic structure for the AChE enzyme complexed with THA is available.[13] On the basis of these structural data, we performed a preliminary modeling study with the new azaheterocyclic compounds **7**−**9** in order to verify the main structural features that determine their binding and to evaluate the interactions observed in the crystallographic structure of the complex THA−AChE. Due to the molecular rigidity of these compounds, only the structure energy of each molecule was minimized and overlaid on the template (THA) using the program Search_Compare within Insight-II.[14] After performing a preliminary molecular dynamic study[15] with AChE, we were also able to identify interactions of the azaheterocyclic ring of the new derivatives **7**−**9** with Phe330 and Trp84 of AChE, as found for the quinoline ring of **6** in the THA−AChE complex. In addition, we observed that for the linear extended isomer **9** there would be supplementary π-stacking interactions and favorable steric access of the NH_2 group to the anionic site of AChE. These results suggested a potential benefit in the overall interactions involving the extended pyrazolo[4,3-*d*]pyridine system of **9** and prompted us to syntesize the new analogues belonging to the pyrazolo[3,4-*b*][1,8]naphthyridine class **12** (Figure 2).

Results and Discussion

Chemistry. The isomeric series of pyrazolo[3,4-*b*]-pyridine derivatives **7** and pyrazolo[4,3-*b*]pyridine derivatives **8** were prepared by classical synthetic methods, exploring 5-chloro-3-methyl-1-phenylpyrazole[16] (**13**) as the common key intermediate, as illustrated in Scheme 1. Initially, key intermediates for the preparation of pyrazolo[3,4-*b*]pyridine derivatives **7** were target. Pyrazole derivative **13** was regioselectively formylated at C-4, using Vilsmeier−Haack conditions,[16] followed by aza-functionalization of C-5, exploring the nucleophilic displacement of chlorine atom by azide anion, catalyzed by the phase transfer agent tetrabutylammonium bromide (TBAB).[17] Chemoselective reduction of the azide group of compound **15** by treatment with iron powder in acidic media[18] furnished *o*-amino aldehyde derivative **16**, which was converted into the corresponding *o*-amino nitrile derivative **17**, by applying the successive oxymation of the formyl group followed by phosphorus oxychloride dehydration of the oxyme moiety[19] (Scheme 1). On the other hand, key intermediates for the pyrazolo[4,3-*b*]pyridine derivatives **8** were constructed through inverse functionalization of the pyrazolyl chloride derivative **13**, which was initially submitted to a regioselective nitration of C-4 at the pyrazole nucleus, by using fuming nitric acid and acetic anhydride under rigid temperature control.[20] Next, nucleophilic heteroaromatic substitution of chlorine atom at C-5 of nitro derivative **18** by cyanide anion, under phase transfer catalysis,[21] followed by chemoselective reduction of the nitro group,[22] furnished the desired *o*-amino nitrile derivative **20**.

The functionalyzed pyrazolo[3,4-*b*]pyridine derivative **21**, precursor of the compounds of pyrazolo[3,4-*b*][1,8]-naphthyridine series **12**, was prepared through one-pot Knovenagel condensation of malononitrile with *o*-amino-aldehyde derivative (**16**) followed by intramolecular cyclization with the vicinal amino group.[21]

The synthesized *o*-amino nitrile derivatives **17**, **20**, **21** and commercial 3-amino-4-cyano-1-phenylpyrazole[23] (**22**) were submitted to the standard Friedlander reaction protocols[24] with cyclopentanone and/or cyclohexanone, using aluminum chloride as Lewis acid, to furnish the title compounds **7**−**9** and **12.** All structures were in agreement with analytical and spectral data.

Pharmacological Assays. To investigate the potential effects specifically in the central nervous system, compounds **7**−**9** and **12** were evaluated as cholinesterase inhibitors in rat brain tissue. The main enzyme form expressed in the brain of rats and humans is the tetramer of T-type subunits which is bound to membranes through a hydrophobic tail.[25,26] Commercially available enzyme preparations from muscle, electric organ, or erythrocytes contain other enzyme forms, which vary in their sensitivity to inhibitors. Concentration−response curves were obtained for all seven new compounds **7**−**9** and **12**, and their mean inhibitory concentration (IC_{50}) was estimated (Table 1). All compounds were fully efficacious in inhibiting brain cholinesterase, as illustrated for compound **12b** in Figure 3. For comparison, THA (**6**) and galanthamine (GAL, **1**) were tested in the same assay conditions, showing mean IC_{50}'s of 0.16 μM and 3.1 μM, respectively. The new THA analogues **7**−**9** and **12** were all less potent than the parent compound (**6**) and could be separated in two groups according to the IC_{50}. Compounds **9** and **12b** showed similar potency, with IC_{50} of 6.01 and 6.39 μM, respectively, comparable to that of GAL (**1**), while compounds **7**−**8** and **12a** fell into another group, with IC_{50}'s ranging from 23.2 μM to 32.2 μM. The most active compounds (**9**, **12b**) were also tested in a rat brain butyrylcholinesterase (BuChE) assay (Table 1). The maximum rate of butyrylthiocholine hydrolysis in the absence of inhibitors was approximately 10% of that of acetylthiocholine hydrolysis when assayed in the same rat brain samples, showing that the total cholinesterase IC_{50} largely reflects AChE inhibition. Compounds **9** and **12b** showed significant selectivity toward AChE, with selectivity indices (SI) of 5.3 and 20.9, respectively, whereas THA (**6**) was less selective, with a SI of 1.5. It must be considered that the substrate concentrations

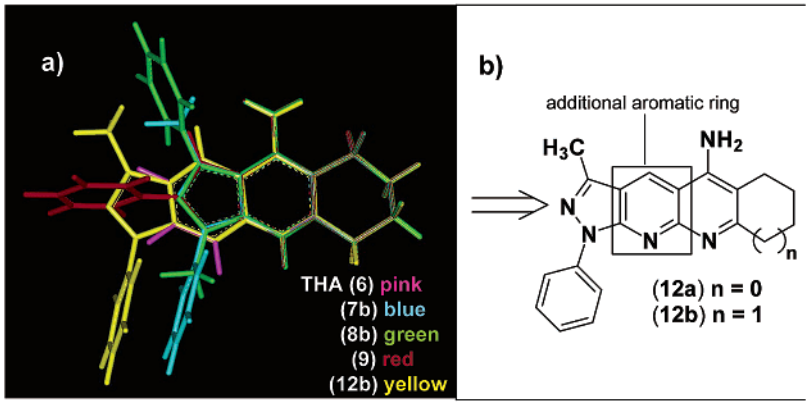

Figure 2. (a) Superimposition of the minimum energy conformers of tacrine (THA, **6**), pyrazolo[4,3-*b*]pyridine derivatives (**7b**, **8b**, **9**) and the tetracyclic analogue (**12b**). (b) Structural design of new pyrazolo[3,4-*b*][1,8]naphthyridine derivatives (**12**).

Scheme 1[a]

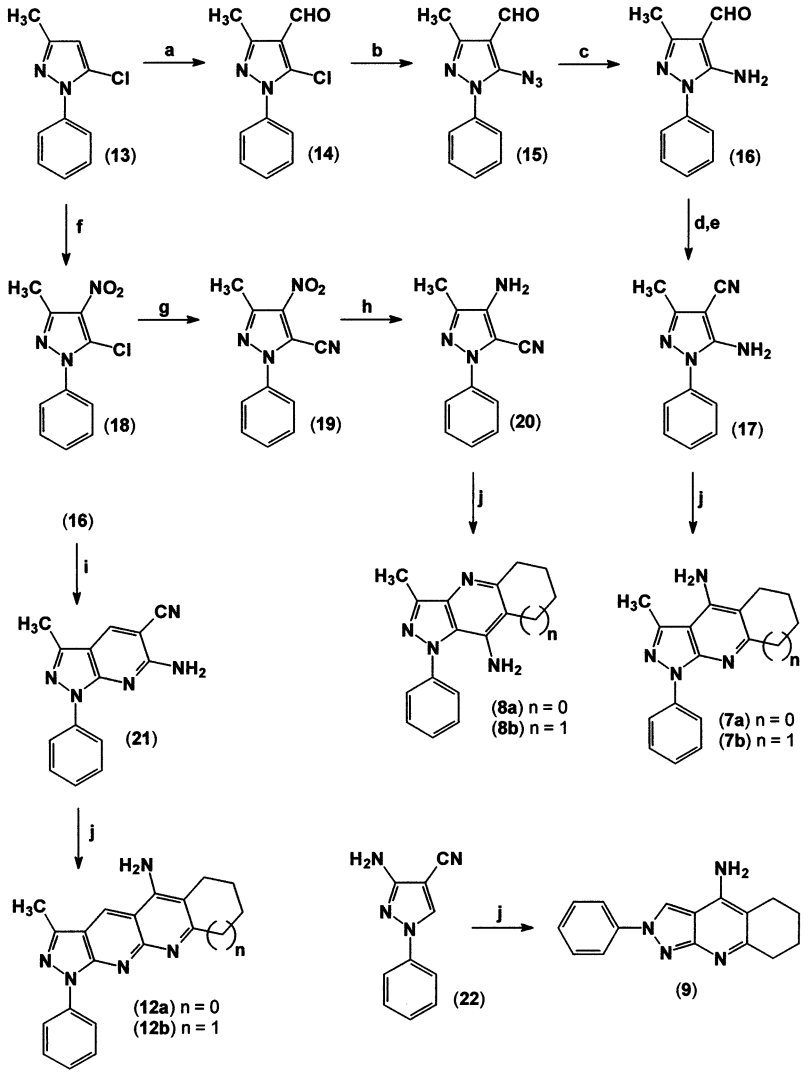

[a] Reagents: (a) $POCl_3$, DMF, 70 °C, 7 h, 85%; (b) NaN_3, TBAB, DMSO, rt, 24 h, 90%; (c) Fe, NH_4Cl, AcOEt/H_2O, rt, 4 h, 92%; (d) $NH_2OH.HCl$, pyridine, EtOH, rt, 2 h, 92%; (e) $POCl_3$, reflux, 30 min, 65%; (f) HNO_3, Ac_2O, 3−5 °C, 1 h, 64%; (g) NaCN, TBAB, DMSO, 80 °C, 16 h, 73%; (h) Fe, NH_4Cl, EtOH/H_2O, reflux, 15 min, 75%; (i) $NCCH_2CN$, Et_3N, MeOH, reflux, 3 h, 72%; (j) cyclopentanone or cyclohexanone, $AlCl_3$, $ClCH_2CH_2Cl$, reflux, 3 h.

used in our assays were high, which is expected to underestimate the potency of competitive inhibitors. Although this had little impact in the IC_{50} of THA, whose inhibition is mostly noncompetitive,[27] it might have affected the novel compounds to an unknown extent. A detailed analysis of mechanism would require further enzyme kinetics studies which are beyond the scope of this paper, but the rankings of IC_{50} and SI among the compounds were deemed adequate for an initial discussion of SAR.

These results clearly indicated that the tetracyclic and the linear extended pyrazolopyridine derivatives **12b**

Table 1. IC_{50} of New THA Analogues (**7**−**9**, **12**), THA (**6**), and Galanthamine (**1**) for Inhibition of Rat Brain Cholinesterases (ChE) (μM)[a]

compound	total ChE[b]	BuChE	SI[c]
THA (**6**)	0.16 ± 0.03 (4)	0.24 ± 0.10 (2)	1.5
7a	31.2 ± 4.2 (2)		
7b	28.5 ± 0.3 (3)		
8a	32.2 ± 4.4 (2)		
8b	26.7 ± 3.1 (3)		
9	6.01 ± 1.22 (3)	31.9 ± 10.1 (2)	5.3
12a	23.2 ± 5.3 (3)		
12b	6.39 ± 0.86 (3)	134 ± 15 (2)	20.9
GAL (**1**)	3.10 ± 0.18 (2)		

[a] Values are means ± SEM of the IC_{50} from the indicated number of animals in parentheses. [b] Total cholinesterase (ChE) and butyrylcholinesterase (BuChE) activities were determined by Ellman's method,[28] as described in the Experimental Section. [c] SI = selectivity index = (IC_{50} BuChE)/(IC_{50} total ChE) ratio.

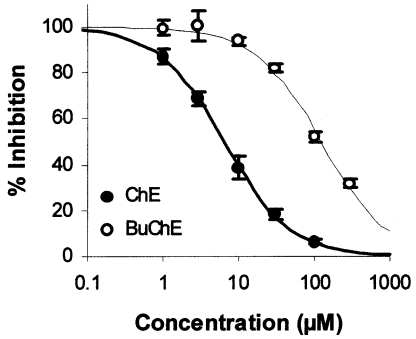

Figure 3. Cholinesterase inhibition curves for compound **12b**. The best-fitting curves had IC_{50}'s of 6.5 and 123.5 μM for total cholinesterase and butyrylcholinesterase, respectively, in these two representative experiments. Data points and error bars are means and SD from three tissue samples.

and **9**, respectively, presented the best inhibitory profile on AChE of this series, with a selectivity index superior to that of THA (**6**). On the other hand, derivatives of the series **7** and **8** were less active, indicating that the *angular* pattern adopted by the *N*-phenyl group attached to the pyrazolopyridine system in these derivatives introduced severe steric constraints into the molecular fit with Ile439/His440 and Tyr334/Trp432 on the active site of AChE. Additionally, the tetracyclic cyclopentane derivative **12a** was four times less potent (IC_{50} = 23.2 μM) than the corresponding cyclohexane derivative **12b** (IC_{50} = 6.39 μM), possibly due to entropic effects related to the more conformationally flexible cyclopentane ring in this compound.

Compounds **7**−**9** and **12** were also tested for their acute neurotoxicity in vitro. Rat cortical neurons in high-density cultures were exposed to compounds **7**−**9** and **12** for 4 h, and the cell damage was evaluated by the release of intracellular lactate dehydrogenase (LDH).[29] In the control conditions, a small amount of LDH was released due to the stress of washing and removal of serum from the culture medium, as shown by the dashed line in Figure 4. Compounds **12a** and **12b** showed a significant concentration-dependent neurotoxicity, being able to kill most cells at 500 μM.

Compound **9** was toxic at 500 μM, but not at 100 μM. In contrast, THA (**6**) (up to 500 μM) was not neurotoxic, suggesting that the mechanisms underlying its well-known acute toxicity to other cell types, particularly hepatocytes,[11,30] were not operative in our assay. This is unexpected, in view of a recent study showing that

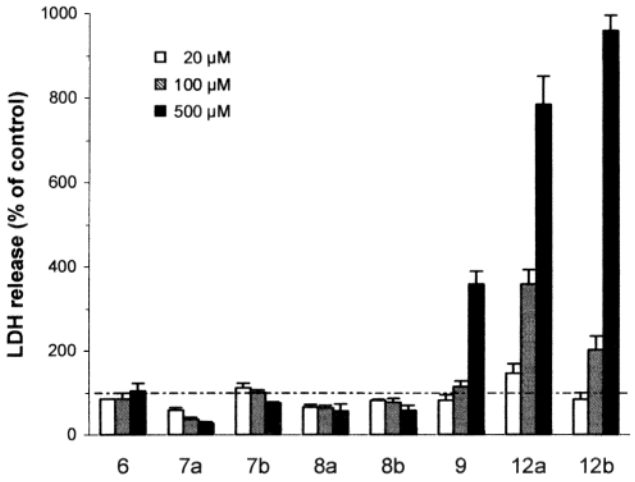

Figure 4. Neurotoxicity of compounds **7**−**9** and **12**, as compared to that of THA (**6**). Rat cortical neurons were exposed to the compounds for 4 h, and cell damage was evaluated by the amount of LDH released. Bar heights and error bars are means and SD from three culture wells. Very similar results were obtained in other two experiments.

THA (**6**) affects membrane fluidity of hepatocytes as early as 30 min after exposure to concentrations above 250 μM, and that this effect might underlie the drug-induced LDH release.[31] It is possible that the distinct composition of neuronal membranes makes them less susceptible to the membrane-destabilizing effect of THA (**6**). The neurotoxic mechanism of compounds **9**, **12a**, and **12b** is unknown at present, and may be unrelated to the cytotoxic mechanisms of THA (**6**). Interestingly, compounds **7**−**8** were not significantly toxic to neurons and actually showed a tendency to reduce LDH release below control levels in a concentration-dependent manner. This possibly neuroprotective effect could be a desirable additional feature in Alzheimer's treatment and is worth further investigation.

Molecular Dynamics Studies. The most active derivatives **9** and **12b** were next studied by molecular dynamics (MD) in order to assess their probable binding mode in the active site of AChE. The active site of AChE is defined by a few key residues: Ser200, His440, Glu327, Phe330, Trp84, Trp432, and Tyr121. The contact distances between most of these residues and the THA (**6**) pharmacophore groups are shorter than 4 Å, involving hydrophobic interactions. Initially, MD simulations were performed in the template THA−AChE, for which the key interactions responsible for the stability of the complex have been determined.[15] After the minimization step, the inhibitor THA (**6**) remains stacked with the aromatic residues Phe330 and Trp84 and is directly hydrogen-bonded to the backbone oxygen atom of His440 through its $^{+}$NH group (Figure 5a) as observed in the crystal structure. Moreover, the NH_2 group of THA (**6**) is hydrogen-bonded to two water molecules (W634 and W643) (Figure 5a). The conformations and interactions achieved were in good agreement with the crystallographic structure of the THA−AChE complex.[13] The model was then used to compare the binding mode of the more active new heterocyclic isosteric derivatives **9** and **12b** with AChE.

The knowledge of the exact binding mode of derivatives **9** and **12b** with AChE could be useful for the optimization of these new lead-compounds. Therefore,

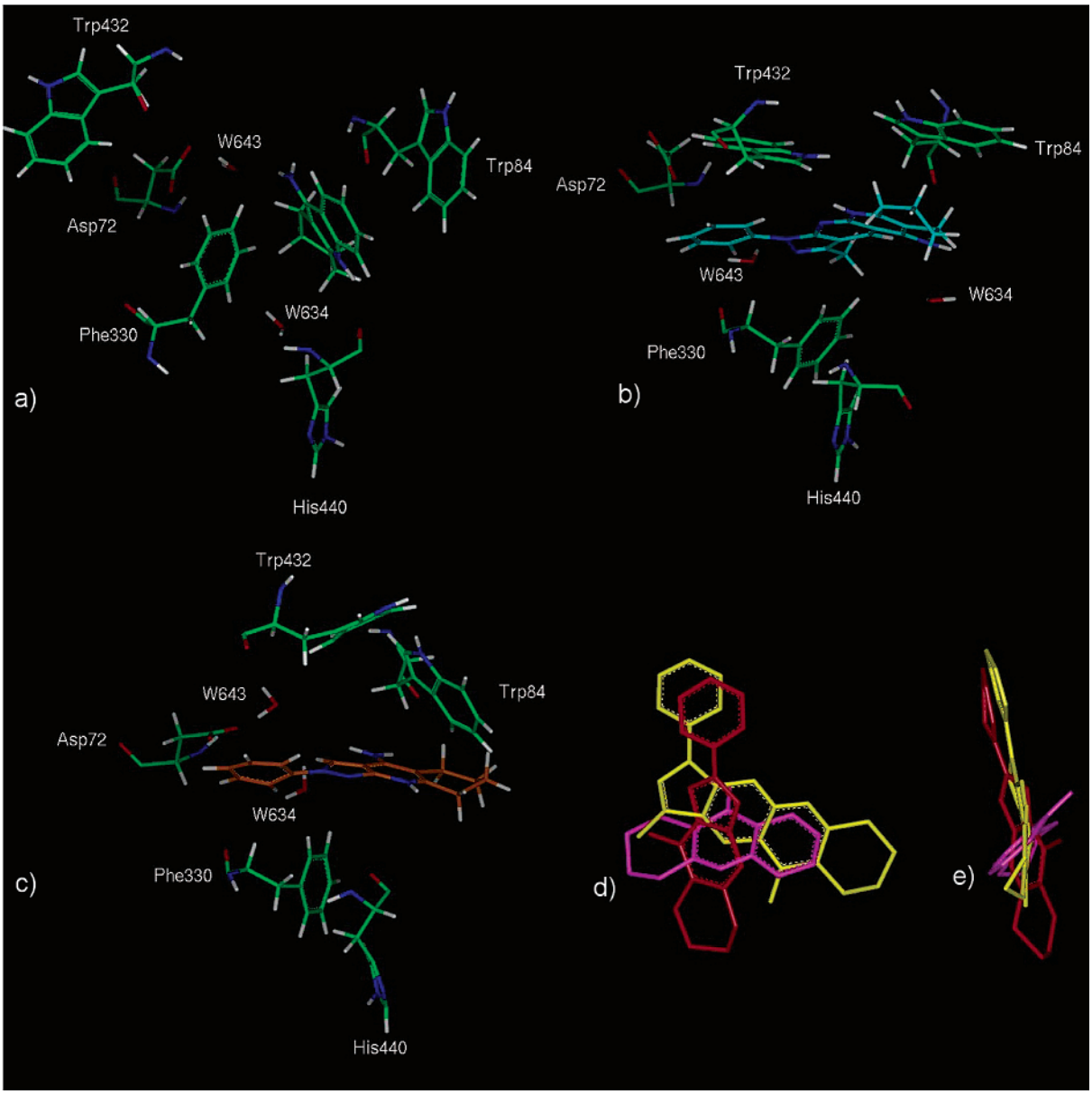

Figure 5. Plots of the main interactions between AChE and (a) THA (**6**); (b) compound **12b**; (c) compound **9**. Superimposition between THA (**6**), **12b**, and **9** positioned in the putative binding mode, (d) frontal view; (e) orthogonal view.

the MD simulation was performed to investigate the stability of the AChE-**12b** and AChE-**9** complexes (Figure 5, parts b and c, respectively) and to examine the occurrence of local structural changes in the residues forming the active site. Further insight into the suitability of the binding model was gained by comparison with the results obtained from THA simulations. Analysis of the collected structures allowed us to determine key interactions between AChE and new THA-isosteres **9** and **12b**. As detailed below, the model developed predicts significant differences between the binding modes of THA and both derivatives **9** and **12b**. Thus, the largest difference was found for the azaheterocyclic ring of **9**, which is orthogonally oriented relative to the 4-aminoquinoline ring of THA (**6**) in the active site of AChE. Therefore, it is likely that the steric demand imposed by some residues in the active site would significantly affect the orientation of the *N*-heterocyclic ring of **9** and **12b** upon binding to AChE. This reorientation changes the pattern of interactions in the binding pocket for both derivatives, so that, for instance, the hydrogen bond observed for **6** with His440 is not observed with either derivative. A T-stacking interaction was observed between the imidazole group of His440 and the pyridine ring of compound **9**, with the imidazolyl-NH oriented toward the phenyl ring of Phe330. However, analysis of the interaction energy with His440 indicated a favorable contribution particularly for derivative **9** (-6.98 ± 0.9 kcal mol^{-1}). The indole ring of Trp84 remained stacking with the pyrazolopyridine ring of compound **9**, as with THA (**6**). This π-stack interaction was lost in the case of derivative **12b**, but was effectively replaced by a hydrogen bond between the carbonyl oxygen atom of Trp84 and the N−H group of **12b** plus van der Waals interactions of the indole ring with the compound's cyclohexane ring. The energy profile of the interaction with Trp84 did not differ among the ligands, i.e., THA (-12.96 ± 1.1 kcal mol^{-1}), **9** (-12.27 ± 1.4 kcal mol^{-1}) and **12b** (-11.11 ± 1.3 kcal mol^{-1}). In addition, the stacking between compound **12b** and

Phe330 occurred with the *N*-phenyl substituent on the pyrazole ring, while in the binding of THA with AChE, this interaction occurs with the quinoline ring. The binding modes of AChE ligands THA (**6**), **12b**, and **9** is depicted in Figure 5.

Conclusions

The new analogues of THA **7**−**12** containing the azaheterocyclic pyrazolo[4,3-*d*]pyridine and pyrazolo-[3,4-*b*][1,8]naphthyridine system have been designed, synthesized, and subjected to pharmacological evaluation. The biological results identify compounds **9** and **12b** as the most active, presenting an IC_{50} of 6.01 and 6.39 μM, respectively, each being a cyclohexane derivative from its *N*-heterocyclic class. In addition, derivative **12b**, was ca. 21 times more selective for acetylcholinesterase over butyrylcholinesterase, presenting a selectivity index ca. 10-fold superior to that of THA (**6**). Compounds **9** and **12b** were toxic to rat cortical neurons only at concentrations 10× above their IC_{50}, and most of the other derivatives were even less neurotoxic, indicating that these new compounds represent useful templates for development of new anti-AD agents.

Experimental Section

Chemistry. Melting points were determined with a Quimis 540 apparatus and are uncorrected. ^{1}H and ^{13}C NMR spectra were determined in deuteriochloroform containing ca. 1% tetramethylsilane as an internal standard with a Brucker DRX 200 spectrometer at 200 and 50 MHz, respectively. Splitting patterns are as follows: s, singlet; d, doublet; br, broad; m, multiplet. ^{1}H and ^{13}C NMR assignments given for each compound were confirmed by HMQC and HMBC experiments. IR spectra were obtained with a Nicolet-550 Magna spectrophotometer using KBr pellets. The mass spectra (MS) were obtained on GC/VG Micromass 12 spectrometer at 70 eV. Ultraviolet (UV) spectra were determined in methanol solution on a Beckmann DU-70 spectrophotometer. Microanalysis data were obtained with a Perkin-Elmer 240 analyzer, using a Perkin-Elmer AD-4 balance. Prior to concentration under reduced pressure, all organic extracts were dried over anhydrous sodium sulfate powder. The progress of all reactions was monitored by TLC performed on 2.0 × 6.0 cm aluminum sheets precoated with silica gel 60 (HF-254, Merck) to a thickness of 0.25 mm. The developed chromatograms were viewed under UV light at 254 nm. For column chromatography Merck silica gel (70−230 mesh) was used. Solvents used in the reactions were dried, redistilled prior to use and stored over +3−4 Å molecular sieves. Reaction mixtures were generally stirred under a dry nitrogen atmosphere.

5-Chloro-3-methyl-1-phenyl-1*H*-pyrazole-4-carbaldehyde (14). The 5-chloro-3-methyl-1-phenyl-1*H*-pyrazole (**13**) (2.21 g, 11.48 mmol) was heated at 70 °C for 7 h with a mixture of phosphorus oxychloride (3.52 g, 22.98 mmol) and *N*,*N*-dimethylformamide (1.6 g, 22.98 mmol) and allowed to cool to 40 °C. Then, cold water (80 mL) was added, followed by neutralization with concentrated aqueous sodium carbonate. The mixture was extracted with dichloromethane (5 × 80 mL), and then organic layers were dried with anhydrous sodium sulfate and concentrated under reduced pressure. The crude solid was purified by recrystallization in ethanol, yielding 2.12 (84%) of the pyrazole-4-carbaldehyde derivative **14**, as yellow needles, mp 131−132 °C (lit.,[32] 132 °C): ^{1}H NMR (200 MHz, $CDCl_3$) δ 2.54 (s, 3H, CH_3), 7.47−7.56 (m, 5H, Ph-H2′, Ph-H3′, Ph-H4′, Ph-H5′ and Ph-H6′), 9.97 (s, 1H, C*H*O); ^{13}C NMR (50 MHz, $CDCl_3$) δ 14.0 (*C*H_3), 117.5 (C4), 125.3 (Ph-C2′ and Ph-C6′), 129.3 (Ph-C4′), 129.4 (Ph-C3′ and Ph-C5′), 137.1 (Ph-C1′), 133.6 (C5), 151.9 (C3), 184.0 (*C*HO); IR (KBr) cm^{-1}: 1676 (C═O).

5-Azido-3-methyl-1-phenyl-1*H*-pyrazole-4-carbaldehyde (15). A mixture of 5-chloro-3-methyl-1-phenyl-1*H*-pyrazole-4-carbaldehyde (**14**) (3.00 g, 13.61 mmol), sodium azide (1.10 g, 16.33 mmol), and tetrabutylammonium bromide (0.526 g, 1.63 mmol) dissolved in 12 mL of DMSO was stirred at room temperature for 24 h. The reaction mixture was poured in ice and the crude precipitate collected by filtration, washed with cooled water, dried, and recrystallized with petroleum ether/dichloromethane mixture to give 2.84 g (92%) of azido compound **15**, as a brown solid, mp 42 °C (lit.,[21] 42−43 °C): ^{1}H NMR (200 MHz, $CDCl_3$) δ 2.52 (s, 3H, CH_3), 7.38−7.51 (m, 3H, Ph-H3′, Ph-H4′ and Ph-H5′), 7.59 (m, 2H, Ph-H2′ and Ph-H6′), 9.94 (s, 1H, C*H*O); ^{13}C NMR (50 MHz, $CDCl_3$) δ 12.9 (*C*H_3), 112.4 (C4), 124.4 (Ph-C2′ and Ph-C6′), 128.7 (Ph-C4′), 129.2 (Ph-C3′ and Ph-C5′), 137.1 (Ph-C1′), 140.6 (C5), 152.2 (C3), 183.8 (*C*HO); IR (KBr) cm^{-1}: 2156 (N═N═N−), 1672 (C═O).

5-Amino-3-methyl-1-phenyl-1*H*-pyrazole-4-carbaldehyde (16). To a mixture of 5-azido-3-methyl-1-phenyl-1*H*-pyrazole-4-carbaldehyde (**15**) (2.80 g, 12.33 mmol), iron powder (2.22 g, 39.6 mmol), and ethyl acetate (10 mL) was added a solution of ammonium chloride (3.52 g, 65.8 mmol) in water (10 mL), and the resulting emulsion was stirred at room temperature for 4 h. The mixture was filtered and the residue washed with ethyl acetate (10 mL). The organic layers were dried with anhydrous sodium sulfate and evaporated under reduced pressure to furnish a crude oily residue. After column chromatography on silica gel using dichloromethane as eluent, 2.4 g (91%) of amino aldehyde derivative **16** was obtained as a white solid, mp 96−97 °C (lit.,[33] 97.5 °C): ^{1}H NMR (200 MHz, $CDCl_3$) δ 2.32 (s, 3H, CH_3), 5.83 (br, 2H, NH_2), 7.28−7.37 (m, 1H, Ph-H4′), 7.42 (m, 4H, Ph-H2′, Ph-H3′, Ph-H5′ and Ph-H6′), 9.60 (s, 1H, C*H*O); ^{13}C NMR (50 MHz, $CDCl_3$) δ 11.8 (*C*H_3), 105.8 (C4), 123.7 (Ph-C2′ and Ph-C6′), 128.2 (Ph-C4′), 129.9 (Ph-C3′ and Ph-C5′), 137.1 (Ph-C1′), 149.3 (C5), 150.8 (C3), 184.0 (*C*HO); IR (KBr) cm^{-1}: 3341 and 3224 (NH_2), 1640 (C═O).

5-Amino-3-methyl-1-phenyl-1*H*-pyrazole-4-carbonitrile (17). A solution of 5-amino-3-methyl-1-phenyl-1*H*-pyrazole-4-carbaldehyde (**16**) (1.0 g, 4.96 mmol) in ethanol (5 mL), maintained at room temperature, was slowly added to a premixed solution of hydroxylamine hydrochloride (0.68 g, 9.9 mmol) and pyridine (0.79 g, 9.9 mmol) and the resulting mixture stirred for 2 h. The reaction mixture was cooled, and the precipitate formed was filtered off and used for the next step without further purification, yielding 0.98 g (92%) of the oxyme intermediate, as an amorphous yellow solid, mp 188−189 °C. Next, 5-amino-3-methyl-1-phenyl-1*H*-5-pyrazole carbaldehyde oxime (0.75 g, 3.46 mmol) was added in small portions to cooled (0 °C) phosphorus oxychloride (6 mL), and the resulting mixture was then carefully refluxed for 30 min. The reaction mixture was cooled, slowly added to ice−water (ca. 50 g), and neutralized with 10% aq sodium carbonate solution. The brown precipitate formed was filtered off and recrystallized from ethanol yielding 0.45 g (65%) of title compound **17** as yellow needles, mp 96 °C: ^{1}H NMR (200 MHz, $CDCl_3$) δ 2.30 (s, 3H, CH_3), 4.69 (br, 2H, NH_2), 7.40−7.54 (m, 5H, Ph-H2′, Ph-H3′, Ph-H4′, Ph-H5′ and Ph-H6′); ^{13}C NMR (50 MHz, $CDCl_3$) δ 13.0 (*C*H_3), 76.3 (C4), 114.7 (*C*N), 124.2 (Ph-C2′ and Ph-C6′), 128.7 (Ph-C4′), 130.0 (Ph-C3′ and Ph-C5′), 137.1 (Ph-C1′), 150.3 (C3), 151.1 (C5); IR (KBr) cm^{-1}: 3334 and 3226 (NH_2), 2218 (CN). Anal. ($C_{11}H_{10}N_4$) C, H, N.

5-Chloro-3-methyl-4-nitro-1-phenyl-1*H*-pyrazole (18). To a solution of 5-chloro-3-methyl-1-phenylpyrazole (**13**) (30 g, 155.7 mmol) in 150 mL of acetic anhydride at 0 °C was added dropwise 30 mL of fuming nitric acid in such a manner that the temperature was maintained at 0−5 °C. After addition of the acid, the temperature of the reaction mixture was allowed to gradually reach 25−30 °C and then was maintained at this temperature for 4 h. At the end of this period the reaction mixture was poured over crushed ice, and the precipitate was filtered and washed with water. After drying, the precipitate was crystallized from ethanol to give 23.8 g (64%) of the compound **18**, as a yellow light crystals, mp 115−116 °C (lit.,[20] 115−116 °C): ^{1}H NMR (200 MHz, $CDCl_3$) δ 2.62 (s, 3H, CH_3), 7.52 (s, 5H, Ph-H2′, Ph-H3′, Ph-H4′, Ph-H5′ and Ph-H6′); ^{13}C

NMR (50 MHz, $CDCl_3$) δ 14.7 (*C*H_3), 125.5 (Ph-C2′ and Ph-C6′), 128.1 (C5), 129.5 (Ph-C3′ and Ph-C5′), 129.9 (Ph-C4′), 136.9 (Ph-C1′), 147.6 (C3); IR (KBr) cm^{-1}: 1542 and 1354 (NO_2).

3-Methyl-4-nitro-1-phenyl-1*H*-pyrazole-5-carbonitrile (19). A mixture of 5-chloro-3-methyl-4-nitro-1-phenyl-1*H*-pyrazole (**18**) (1.18 g, 5.1 mmol), sodium cyanide (0.27 g, 5.5 mmol), and tetrabutylammonium bromide (0.177 g, 0.55 mmol) dissolved in 6 mL of DMSO was stirred at 80 °C for 16 h. The reaction mixture was poured in ice and the solid collected by vacuum filtration in a Büchner, washed with cooled water, dried, and used in the next step without further purification, yielding 0.83 g (73%) of cyanide derivative **19**, as a light brown solid, mp 126−128 °C: ^{1}H NMR (200 MHz, $CDCl_3$) δ 2.69 (s, 3H, C*H*$_3$), 7.60 (m, 3H, Ph-H3′, Ph-H4′ and Ph-H5′), 7.71 (m, 2H, Ph-H2′ and Ph-H6′); ^{13}C NMR (50 MHz, $CDCl_3$) δ 13.6 (*C*H_3), 108.0 (*C*N), 113.4 (C5), 118.2 (C3), 123.4 (Ph-C2′ and Ph-C6′), 130.0 (Ph-C3′ and Ph-C5′), 130.6 (Ph-C4′), 137.3 (Ph-C1′), 147.4 (C4); IR (KBr) cm^{-1}: 2245 (CN), 1502 and 1360 (NO_2). Anal. ($C_{11}H_8N_4O_2$) C, H, N.

4-Amino-3-methyl-1-phenyl-1*H*-pyrazole-5-carbonitrile (20). A mixture of 3-methyl-4-nitro-1-phenyl-1*H*-pyrazole-5-carbonitrile (**19**) (1.0 g, 4.38 mmol), iron powder (0.74 g, 13.15 atg), and ammonium chloride (1.16 g, 21.9 mmol) in 30 mL of a mixture of ethanol and water (2:1) was refluxed for 15 min. Then, the reaction mixture was filtered hot, and the filtrate was evaporated to half of its original volume. After being cooled with an ice bath for 2 h, the yellow crystals of amino compound **20** (0.65 g, 75%) were collected by filtration, mp 112−114 °C. ^{1}H NMR (200 MHz, $CDCl_3$) δ 2.26 (s, 3H, C*H*$_3$), 3.64 (br, 2H, N*H*$_2$), 7.34 (m, 1H, Ph-C4′), 7.46 (m, 2H, Ph-H3′ and Ph-H5′), 7.46 (m, 2H, Ph-H2′ and Ph-H6′); ^{13}C NMR (50 MHz, $CDCl_3$) δ 10.7 (*C*H_3), 99.8 (C4), 112.0 (*C*N), 121.2 (Ph-C2′ and Ph-C6′), 127.4 (Ph-C4′), 129.6 (Ph-C3′ and Ph-C5′), 138.9 (Ph-C1′), 139.2 (C5); IR (KBr) cm^{-1}: 3357 and 3323 (NH), 2223 (CN). Anal. ($C_{11}H_{10}N_4$) C, H, N.

6-Amino-3-methyl-1-phenyl-1*H*-pyrazolo[3,4-*b*]pyridine-5-carbonitrile (21). A solution of 5-amino-3-methyl-1-phenyl-1*H*-pyrazole-4-carbaldehyde (**16**) (0.5 g, 2.5 mmol), malononitrile (0.17 mL, 2.6 mmol), and triethylamine (6 drops) in methanol (15 mL) was refluxed on steam bath for 2 h. The white colored product obtained after cooling was filtered off and recrystallized from methanol, yielding 0.44 g (70%) of the desired fused heterocycle derivative **21**, mp 223−225 °C (lit.,[21] 226 °C); ^{1}H NMR (200 MHz, $CDCl_3$) δ 2.56 (s, 3H, C*H*$_3$), 5.72 (br, 2H, N*H*$_2$), 7.19 (t, J = 7.4 Hz, 1H, Ph-H4′), 7.39 (t, J = 8.0 Hz, 2H, Ph-H3′ and Ph-H5′), 8.00 (s, 1H, Pyridine-H4), 8.05 (d, J = 8.4 Hz, 2H, Ph-H2′ and Ph-H6′); ^{13}C NMR (50 MHz, $CDCl_3$) δ 12.2 (*C*H_3), 87.6 (C5), 110.2 (C3a), 117.2 (*C*N), 121.0 (Ph-C2′ and Ph-C6′), 125.8 (Ph-C4′), 128.8 (Ph-C3′ and Ph-C5′), 136.5 (C4), 138.8 (Ph-C1′), 143.9 (C3), 151.0 (C7a), 158.2 (C6); IR (KBr) cm^{-1}: 3331 and 3219 (NH), 2210 (CN).

General Procedure for the Preparation of the Tacrine Analogues 7−9 and 12. A mixture of 0.5 mmol of the corresponding *o*-amino-heteroaryl nitrile derivative **17**, **20**, **21**, or **22** and 1.1 equiv of cyclohexanone or cyclopentanone was added to a suspension of anhydrous aluminum chloride (0.5 mmol) in 15 mL of dry 1,2-dichloroethane, under inert atmosphere, and the reaction mixture was heated at reflux for 3 h. Then, a mixture of THF (3 mL) and water (1 mL) was added, and the reaction mixture was refluxed for additional 10 min and neutralized with 10% aq NaOH solution. After cooling, the organic components were extracted with chloroform and the organic layers were combined, dried, and evaporated at reduced pressure to give the desired azaheterocyclic product. The products were purified by SiO_2 flash chromatography using as eluent a mixture of MeOH/EtOAc/$CHCl_3$/Et_3N (1:2:7:1).

3-Methyl-1-phenyl-1,5,6,7-tetrahydrocyclopenta[*b*]pyrazolo[4,3-*e*]pyridin-4-amine (7a). Compound **7a** was obtained in 38% yield, from Friedländer condensation of the 4-amino-3-methyl-1-phenyl-1*H*-pyrazole-5-carbonitrile (**20**) with cyclopentanone, as a yellow solid, mp 135−6 °C; ^{1}H NMR (200 MHz, $CDCl_3$) δ 2.11 (qt, J = 6.9 Hz, 2H, C6*H*$_2$), 2.67 (s, 3H, C*H*$_3$), 2.75 (t, J = 7.0 Hz, 2H, C5*H*$_2$), 3.04 (t, J = 7.0 Hz, 2H, C7*H*$_2$), 4.58 (br, 2H, N*H*$_2$), 7.21 (t, J = 7.1 Hz, 1H, Ph-H4′), 7.44 (t, J = 7.1 Hz, 2H, Ph-H3′ and Ph-H5′), 8.19 (d, J = 7.9 Hz, 2H, Ph-H2′ and Ph-H6′); ^{13}CNMR (50 MHz, $CDCl_3$) δ 15.3 (*C*H_3), 23.6 (C6), 26.4 (C5), 34.7 (C7), 104.8 (C3a), 112.5 (C4a), 121.2 (Ph-C2′ and Ph-C6′), 125.1 (Ph-C4′), 129.0 (Ph-C3′ and Ph-C5′), 140.3 (Ph-C1′), 140.6 (C3), 144.1 (C4), 153.6 (C8a), 167.8 (C7a); IR (KBr) cm^{-1}: 3482 and 3380 (NH), 2922 and 2853 (CH aliph.), 1619 and 1566 (C=N ring); UV (EtOH) λ_{max}: 217 (log ϵ = 4.37), 255 (log ϵ = 4.27), 314 (log ϵ = 4.0). Anal. ($C_{16}H_{16}N_4$) C, H, N.

3-Methyl-1-phenyl-5,6,7,8-tetrahydro-1H-pyrazolo[3,4-*b*]quinolin-4-amine (7b): Compound **7b** was obtained in 42% yield, from Friedländer condensation of the 4-amino-3-methyl-1-phenyl-1*H*-pyrazole-5-carbonitrile (**20**) with cyclohexanone, as a yellow solid, mp 136−8 °C; ^{1}H NMR (200 MHz, $CDCl_3$) δ 1.76−1.79 (m, 4H, C6*H*$_2$ and C7*H*$_2$), 2.32−2.35 (m, 2H, C8*H*$_2$), 2.58 (s, 3H, C*H*$_3$), 2.84−2.86 (m, 2H, C5*H*$_2$), 4.45 (br, 2H, N*H*$_2$), 7.09 (t, J = 7.3 Hz, 1H, Ph-H4′), 7.35 (t, J = 7.5 Hz, 2H, Ph-H3′ and Ph-H5′), 8.20 (d, J = 7.8 Hz, 2H, Ph-H2′ and Ph-H6′); ^{13}CNMR (50 MHz, $CDCl_3$) δ 15.4 (*C*H_3), 22.8 (C8), 23.0 (C6 and C7), 34.3 (C5), 104.4 (C3a), 107.6 (C4a), 120.6 (Ph-C2′ and Ph-C6′), 124.8 (Ph-C4′), 128.9 (Ph-C3′ and Ph-C5′), 140.3 (Ph-C1′), 140.5 (C3), 146.2 (C4), 151.3 (C9a), 158.5 (C8a); IR (KBr) cm^{-1}: 3446 and 3298 (NH), 2930 (CH aliph.), 1643 and 1598 (C=N ring); UV (EtOH) λ_{max}: 218 (log ϵ = 4.33), 254 (log ϵ = 4.23), 316 (log ϵ = 3.9). Anal. ($C_{17}H_{18}N_4$) C, H, N.

3-Methyl-1-phenyl-1,5,6,7-tetrahydrocyclopenta[*b*]pyrazolo[3,4-*e*]pyridin-8-amine (8a). Compound **8a** was obtained in 40% yield, from Friedländer condensation of the 5-amino-3-methyl-1-phenyl-1*H*-pyrazole-4-carbonitrile (**17**) with cyclopentanone, as a yellow solid, mp 173−5 °C; ^{1}H NMR (200 MHz, $CDCl_3$) δ 2.22 (qt, J = 7 Hz, 2H, C6*H*$_2$), 2.6 (s, 3H, C*H*$_3$), 2.76 (t, J = 7 Hz, 2H, C7*H*$_2$), 3.08 (t, J = 7 Hz, 2H, C5*H*$_2$), 4.03 (br, 2H, N*H*$_2$), 7.29−7.41 (m, 1H, Ph-H4′), 7.43−7.50 (m, 4H, Ph-H2′, Ph-H3′, Ph-H5′ and Ph-H6′); ^{13}CNMR (50 MHz, $CDCl_3$) δ 11.2 (*C*H_3), 23.6 (C6), 27.0 (C7), 34.4 (C5), 117.2 (C7a), 123.1 (C3a), 125.7 (Ph-C2′ and Ph-C6′), 127.9 (Ph-C4′), 129.4 (Ph-C3′ and Ph-C5′), 134.47 (C8), 140.5 (Ph-C1′), 142.8 (C8a), 144.1 (C3), 163.4 (C4a); IR (KBr) cm^{-1}: 3496 and 3409 (NH), 2923 and 2859 (CH aliph.), 1625 and 1592 (C=N ring); UV (EtOH) λ_{max}: 226 (log ϵ = 4.57), 256 ((log ϵ = 4.26), 308 (log ϵ = 4.14). Anal. ($C_{16}H_{16}N_4$) C, H, N.

3-methyl-1-phenyl-5,6,7,8-tetrahydro-1H-pyrazolo[4,3-*b*]quinolin-9-amine (8b): Compound **8b** was obtained in 45% yield, from Friedländer condensation of the 5-amino-3-methyl-1-phenyl-1*H*-pyrazole-4-carbonitrile (**17**) with cyclohexanone, as a yellow solid, mp 173−5 °C; ^{1}H NMR (200 MHz, $CDCl_3$) δ 1.87−1.89 (m, 4H, C6*H*$_2$ and C7*H*$_2$), 2.48−2.50 (m, 2H, C5*H*$_2$), 2.64 (s, 3H, C*H*$_3$), 3.01−3.03 (m, 2H, C8*H*$_2$), 4.12 (br, 2H, N*H*$_2$), 7.36−7.41 (m, 1H, Ph-H4′), 7.42−7.51 (m, 4H, Ph-H2′, Ph-H3′, Ph-H5′ and Ph-H6′); ^{13}CNMR (50 MHz, $CDCl_3$) δ 11.2 (*C*H_3), 22.9 (C7), 23.1 (C6), 23.6 (C8), 33.8 (C5), 111.8 (C8a), 123.0 (C3a), 125.7 (Ph-C2′ and Ph-C6′), 127.9 (Ph-C4′), 129.4 (Ph-C3′ and Ph-C5′), 136.3 (C9a), 140.3 (Ph-C1′), 140.4 (C9), 144.2 (C3), 154.4 (C4a); IR (KBr) cm^{-1}: 3481 and 3379 (NH), 2948 and 2881 (CH aliph.), 1619 and 1566 (C=N ring); UV (EtOH) λ_{max}: 223 (log ϵ = 4.52), 255 (log ϵ = 4.21), 306 (log ϵ = 4.10). Anal. ($C_{17}H_{18}N_4$) C, H, N.

2-Phenyl-5,6,7,8-tetrahydro-2*H*-pyrazolo[3,4-*b*]quinolin-4-amine (9): Compound **9** was obtained in 45% yield, from Friedländer condensation of the 3-amino-1-phenyl-1H-pyrazole-4-carbonitrile[22] (**22**) with cyclohexanone, as a yellow solid, mp 215−6 °C; ^{1}H NMR (200 MHz, $CDCl_3$) δ 1.74−1,77 (m, 4H, C6*H*$_2$ and C7*H*$_2$), 2.49−2.51 (m, 2H, C5*H*), 2.75−2.78 (m, 2H, C8*H*$_2$), 6.52 (br, 2H, N*H*$_2$), 7.40 (t, J = 7.2, 1H, Ph-H4′), 7.57 (t, J = 7.6 Hz, 2H, Ph-H3′ and Ph-H5′), 7.90 (d, J = 7.7 Hz, 2H, Ph-H2′ and Ph-H6′), 8.94 (s, 1H, C4*H*); ^{13}CNMR (50 MHz, $CDCl_3$) δ 23.3 (C6), 23.4 (C7), 23.7 (C5), 34.7 (C8), 104.5 (C4a), 108.0 (C3a), 120.0 (Ph-C2′ and Ph-C6′), 120.0 (C3), 127.9 (Ph-C4′), 130.3 (Ph-C3′ and Ph-C5′), 140.6 (Ph-C1′), 146.8 (C4), 159.0 (C9a), 152.2 (C10a), 161.2 (C8a); IR (KBr) cm^{-1}: 3419 and 3306 (NH), 2927 and 2859 (CH aliph.), 1639 and

1552 (C═N ring); UV (EtOH) λ_{max}: 208 (log $\epsilon = 4.52$), 240 (log $\epsilon = 4.40$), 303 (log $\epsilon = 4.37$), 342 (log $\epsilon = 4.00$). Anal. ($C_{16}H_{16}N_4$) C, H, N.

3-Methyl-1-phenyl-1,6,7,8-tetrahydrocyclopenta[*b*]pyrazolo[4,3-*g*][1,8]naphthyridin-5-amine (12a): Compound **12a** was obtained in 45% yield, from Friedländer condensation of the 6-amino-3-methyl-1-phenyl-1H-pyrazolo[3,4-b]pyridine-5-carbonitrile (**21**) with cyclopentanone, as a yellow solid, mp 220−2 °C; ^{1}H NMR (200 MHz, $CDCl_3$) δ 1.95 (qt, $J = 7.1$ Hz, 2H, C*7*H_2), 2.50 (s, 3H, CH_3), 2.70 (t, $J = 7$ Hz, 2H, C*6*H_2), 2.82 (t, $J = 7.5$ Hz, 2H, C*8*H_2), 6.93 (br, 2H, NH_2), 7.12 (t, $J = 7.3$, 1H, Ph-H4′), 7.40 (t, $J = 7.6$ Hz, 2H, Ph-H3′ and Ph-H5′), 8.32 (d, $J = 7.3$ Hz, 2H, Ph-H2′ and Ph-H6′), 9.11 (s, 1H, C*4H*); ^{13}CNMR (50 MHz, $CDCl_3$) δ 12.3 (*C*H_3), 21.7 (C7), 27.3 (C6), 34.9 (C8), 108.3 (C4a), 111.5 (C5a), 115.1 (C3a), 118.8 (Ph-C2′ and Ph-C6′), 124.3 (Ph-C4′), 126.6 (C4), 128.8 (Ph-C3′ and Ph-C5′), 139.5 (Ph-C1′), 143.8 (C3), 148.7 (C5), 150.5 (C10a), 155.5 (C9a), 171.6 (C8a); IR (KBr) cm^{-1}: 3360 and 3224 (NH), 2958 and 2923 (CH aliph.), 1644 and 1598 (C═N ring); UV (EtOH) λ_{max}: 218 (log $\epsilon = 4.16$), 276 (log $\epsilon = 4.55$), 344 (log $\epsilon = 3.75$). Anal. ($C_{19}H_{17}N_5$) C, H, N.

3-Methyl-1-phenyl-6,7,8,9-tetrahydro-1*H*-benzo[*b*]pyrazolo[4,3-*g*][1,8]naphthyridin-5-amine (12b): Compound **12b** was obtained in 52% yield, from Friedländer condensation of the 6-amino-3-methyl-1-phenyl-1H-pyrazolo[3,4-*b*]pyridine-5-carbonitrile (**21**) with cyclohexanone, as a yellow solid, mp 215−6 °C; ^{1}H NMR (200 MHz, $CDCl_3$) δ 1.82−1,87 (m, 4H, C*7*H_2 and C*8*H_2), 2.52−2.56 (m, 2H, C*6*H_2), 2.66 (s, 3H, CH_3), 2.89−2.91 (m, 2H, C*9*H_2), 7.14 (br, 2H, NH_2), 7.27 (t, $J = 7.3$, 1H, Ph-H4′), 7.54 (t, $J = 7.7$ Hz, 2H, Ph-H3′ and Ph-H5′), 8.45 (d, $J = 7.9$ Hz, 2H, Ph-H2′ and Ph-H6′), 9.33 (s, 1H, C*4H*); ^{13}CNMR (50 MHz, $CDCl_3$) δ 12.8 (*C*H_3), 22.6 (C7 and C8), 23.7 (C6), 33.7 (C9), 107.8 (C5a), 108.3 (C4a), 116.1 (C3a), 119.4 (Ph-C2′ and Ph-C6′), 124.9 (Ph-C4′), 127.5 (C4), 129.4 (Ph-C3′ and Ph-C5′), 140.0 (Ph-C1′), 144.6 (C3), 151.3 (C11a), 152.2 (C10a), 153.2 (C5), 162.4 (C9a); IR (KBr) cm^{-1}: 3359 and 3221 (NH), 2956 and 2923 (CH aliph.), 1630 and 1600 (C═N ring); UV (EtOH) λ_{max}: 218 (log $\epsilon = 4.16$), 277 (log $\epsilon = 4.52$), 349 (log $\epsilon = 3.86$). Anal. ($C_{20}H_{19}N_5$) C, H, N.

Molecular Modeling. Molecular Dynamics. We selected the crystal monomeric structure of the AChE-THA complex, including crystal waters, from Protein Data Bank (PDB code: 1ACJ). The hydrogen atoms were added in this structure and energy minimized with 2500 steps of steepest descent followed by 5000 steps of conjugate gradient until a gradient norm of 0.01 kcal mol^{-1} Å^{-1}, keeping all heavy atoms fixed. All residues and crystal waters beyond a region of 16 Å centered on the nitrogen of the pyridine ring were discarded. The missing side chains of some residues inside this region were reconstructed. Acetyl and *N*-methylamide blocking groups were used to cap the truncation points. We assumed that the THA molecule and its derivatives were all protonated. These molecules, ab initio optimized with the 6-31G** basis set, were placed in the active site of the enzyme trough the superimposition of their structures with the THA crystal coordinates. Charges for THA and its derivatives used in MD simulations were fitted to the 6-31G** eletrostatic potential using the CHELPG methodology within PC−SPARTAN−PRO 1.0.5, Wavefunction. To relax some poor interatomic contacts, all complexes formed were energy minimized with 5000 steps of steepest descent followed by 10000 steps of conjugate gradient until a gradient norm of 0.01 kcal mol^{-1} Å^{-1}.

These systems were equilibrated at 300 K for 300 ps using the velocity scaling method to control the temperature. For the production phase the temperature was controlled using the Berendsen method during 300 ps. We used the time step of 1 fs for the dynamics and a nonbonded interaction cutoff radius of 11 Å; the trajectory was sampled every 1 ps. The *leapfrog* algorithm was used for integrating the equations of motion. During the MD simulation the methyl carbon atoms of acetyl and *N*-methylamide blocking groups were kept fixed in order to avoid anomalous behavior due the absence of the discarded residues. To prevent water evaporation, we applied a half-harmonic potential ($k = 0.5$ kcal mol^{-1} Å^{-2}) if the distance from a water oxygen atom to the sphere center exceeded 16 Å. The minimization and MD simulation steps were accomplished using the CVFF force field within the Discover program of the InsightII environment. All calculations were performed on a Silicon Graphics O2 R10000 workstation under Irix operational system.

Pharmacology. Cholinesterase Activity Assays. Ellman's colorimetric method[28] was adapted for determination of total cholinesterase and butyrylcholinesterase activities in rat brain homogenates. Brain tissue from adult Wistar rats was homogenized at 2% w/v (or 10%, for butyrylcholinesterase) in 0.1 M sodium phosphate buffer, pH 7.4, with added NaCl 58.5 g/L and Triton X-100 0.05% v/v. Aliquots of homogenate (20 μL) were incubated with anticholinesterase compounds for 10 min in phosphate buffer pH 8.0 before addition of 5,5′-dithiobis(2-nitrobenzoic) acid and either 1 mM acetylthiocholine iodide or 10 mM butyrylthiocholine iodide (Sigma, St. Louis, MO). The reaction was run at room temperature (22−25 °C) in a final volume of 235 μL in 96-well microplates and was followed at 412 nm for 5 min with a plate reader (SpectraMAX 250, Molecular Devices, Sunnyvale, CA). In every experiment, cholinesterase-independent (nonspecific) substrate hydrolysis was determined by including one experimental group treated with tacrine 20 μM; appropriate tissue and reagent blanks were also included. Reaction velocities were determined in three or four replicates per condition; these were averaged and expressed as percent activity relative to control (solvent), after subtracting the rate of nonspecific hydrolysis. All compounds were tested in at least five concentrations that covered the range producing less than 20% and greater than 80% inhibition, but limited to 500 μM. The IC_{50} based on a single-site model was determined by nonlinear regression. Results are reported as mean ± SEM of IC_{50} obtained independently from two to four animals.

Neurotoxicity. Cortical neurons from Wistar rat fetuses at 18−20 days of gestation were isolated by trypsinization and trituration. Cells were seeded onto poly-L-lysine-coated 24-well plates at a density of four cerebral hemispheres per plate and were maintained in culture in serum-supplemented minimum essential medium (MEM, Gibco, Rockville, MD). Glial cell proliferation was halted by addition of 5-fluoro-2′-deoxyuridine on the day after plating, and neurons were allowed to mature for 14−18 days before the experiments. Cells were washed with serum-free medium, the test compounds were added, and the plates returned to the incubator at 35 °C for 4 h. At the end of this incubation period, neurotoxicity was measured by the amount of LDH released in the culture supernatant.[29] The enzyme's V_{max} was determined kinetically at 37 °C using reagents from a commercial LDH assay kit (Doles Reagentes, Brazil) based on the method of Whitaker.[34] The reaction was run in a final volume of 100 μL in 96-well plates and was followed at 510 nm for 5 min. Results are reported as mean ± SEM of the V_{max} from three culture wells treated in parallel.

Acknowledgment. We gratefully acknowledge financial support and fellowships from the PRONEX (Grant #0888, Brazil), the CNPq (Grants 460.200/00-3 and 50.0033/95-0, Brazil), the FAPERJ (Grant #E−26/170.399/2000, Brazil), the CAPES (Brazil) and the FUJB (Brazil). We also thank the NPPN Analytical Center of Universidade Federal do Rio de Janeiro (Brazil) for spectroscopic facilities.

References

(1) Dolmella, A.; Bandoli, G.; Nicolini, M. Alzheimer's Disease: A Pharmacological Challenge. *Adv. Drug Res.* **1994**, *25*, 202−294.
(2) Weinstock, M. The Pharmacotherapy of Alzheimer's Disease Based on the Cholinergic Hypothesis: An Update. *Neurodegeneration* **1995**, *4*, 349−356.
(3) Gualtieri, F. Cholinergic Receptors and Neurodegenerative Diseases. *Pharm. Acta Helv.* **2000**, *74*, 85−89.
(4) McGleenon, B. M.; Dynan, K. B.; Passmore A. P. Acetylcholinesterase Inhibitors in Alzheimer's Disease. *Br. J. Pharmacol.* **1999**, *48*, 471−480.

(5) Coyle, J.; Kershaw, P. Galanthamine, a Cholinesterase Inhibitor that Allosterically Modulates Nicotinic Receptors: Effects on the Course of Alzheimer's Disease. *Biol. Psych.* **2001**, *49*, 289−299.
(6) Maelicke, A.; Albuquerque, E. X. New Approach to Drug Therapy in Alzheimer's Dementia. *Drug Discovery Today* **1996**, *1*, 53−59.
(7) Greenlee, W.; Clader, J.; Asberom, T.; McCombie, S.; Ford, J.; Guzik, H.; Kozlowski, J.; Li, S.; Liu, C.; Lowe, D.; Vice, S.; Zhao, H.; Zhou, G.; Billard, W.; Binch, H.; Crosby, R.; Duffy, R.; Lachowicz, J.; Coffin, V.; Watkins, R. Ruperto, V.; Strader, C.; Taylor, L.; Cox, K. Muscarinic Agonists and Antagonist in the Treatment of Alzheimer's Disease. *Il Farmaco* **2001**, *56*, 247−250.
(8) Benzi, G.; Moretti, A. Is There a Rationale for the Use of Acetylcholinesterase Inhibitors in the Therapy of Alzheimer's Disease? *Eur. J. Pharmacol.* **1998**, *346*, 1−13.
(9) Gracon, S. I.; Knapp, M. J.; Berghoff, W. G.; Pierce, M.; DeJong, R.; Lobbestael, S. J.; Symons, J.; Dombey, S. L.; Luscombe, F. A.; Kraemer, D. Safety of Tacrine: Clinical Trials, Treatment IND, and Postamarketing Experience. *Alzheimer Dis. Assoc. Disord.* **1998**, *12*, 93−101.
(10) Balson, R.; Gibson, P. R.; Ames, D.; Bhathal, P. S. Tacrine-Induced Hepatotoxicity. Tolerability and Management. *CNS Drugs* **1995**, *4*, 168−181.
(11) Stachlewitz, R. F.; Arteel, G. E.; Raleigh, J. A.; Connor, H. D.; Mason, R. P.; Thurman, R. G. Development and Characterization of a New Model of Tacrine-Induced Hepatotoxicity: Role of the Sympathetic Nervous System and Hypoxia-Reoxygenation. *J. Pharmacol. Exp. Ther.* **1997**, *282*, 1591−1599.
(12) Dias, R. S.; Freitas, A. C. C.; Barreiro, E. J.; Goins, D. K.; Nanayakkara, D.; McChesney, J. D. Synthesis and Biological Activity of New Potential Antimalarial: 1H-pyrazolo[3,4-b]-pyridine derivatives. *Boll. Chim. Farm.* **2000**, *139*, 14−20.
(13) Entry 1ACJ in the PDB (www.rcsb.org/pdb) for the complex of AChE with THA was utilized in molecular modeling studies.
(14) Insight-II: Biosym Technologies: San Diego, 1993.
(15) Wlodek, S. T.; Clark, T. W.; Scott, L. R.; McCammon, J. A. Molecular Dynamics of Acetylcholinesterase Dimer Complexed with Tacrine. *J. Am. Chem. Soc.* **1997**, *119*, 9513−9522.
(16) Wallace, D. J.; Straley, J. M. Synthesis of 5-Oxo-2-pyrazoline-4-carboxaldehyde. *J. Org. Chem.* **1961**, *26*, 3825−3826.
(17) Becher, J.; Jorgensen, P. L.; Pluta, K.; Krake, N. J.; Fält-Hansen, B. Azide Ring-Opening-Ring-Closure Reactions and Tele-substitutions in Vicinal Azidopyrazole, Pyrrole- and Indole-carboxaldehydes. *J. Org. Chem.* **1992**, *57*, 2127−2134.
(18) Cho, S.; Choi, W.; Lee, S.; Yoon, Y.; Shin, S. C. Chemoselective Reduction of Highly functionalyzed Azidopyridazines to Corresponding Aminopyridazines Using Fe/NH_4Cl in Organic Sovent-Water Two-phase Solution. *Tetrahedron Lett.* **1996**, *37*, 7059−7060.
(19) Iddon, B.; Khan, N.; Lim, B. L. Azoles. Part 7. A Convenient Synthesis of Thieno[2,3-d]imidazoles. *J. Chem Soc., Perkin Trans. 1* **1987**, 1457−1463.
(20) Khan, M. A.; Freitas, A. C. C. Hetarylpyrazoles. IV (1). Synthesis and Reactions of 1, 5′-Bipyrazoles. *J. Heterocycl. Chem.* **1983**, *20*, 277−279.
(21) Ahluwalia, V. K.; Goyal, B. A Facile Synthesis of Pyrazolo[3,4-*b*]pyridines. *Synth. Commun.* **1996,** *26*, 1341−1348.
(22) Lages, A. S.; Silva, K. C. M.; Miranda, A. L. P.; Fraga, C. A. M.; Barreiro, E. J. Synthesis and Pharmacological Evaluation of New Flosulide Analogues, Synthesized from Natural Safrole. *Bioorg. Med. Chem. Lett.* **1998**, *8*, 183−188.
(23) Purchased from Aldrich Co., Milwaukee, WI.
(24) (a) Rios, C.; Marco, J. L.; Carreiras, M. D. C.; Chinchón, P. M.; Garcia, A. G.; Villarroya, M. Novel Tacrine Derivatives that Block Neuronal Calcium Channels. *Bioorg. Med. Chem. Lett.* **2002**, *10*, 2077−2088. (b) Martinez-Grau, A.; Marco, J. L. Friedländer Reaction of 2-Amino-3-Cyano-4*H*-Pyrans: Synthesis of Derivatives of 4*H*-Pyran[2, 3-*b*]Quinoline, New Tacrine Analogues. *Bioorg. Med. Chem. Lett.* **1997,** *7*, 3165−3170. (c) McKeena, M. T.; Proctor, G. R.; Young, L. C.; Harvey, A. L. Novel Tacrine Analogues for Potential Use against Alzheimer's Disease: Potent and Selective Acetylcholinesterase Inhibitors and 5-HT Uptake Inhibitors. *J. Med. Chem.* **1997**, *40*, 3515−3523.
(25) Boschetti, N.; Liao, J.; Brodbeck, U. The Membrane Form of Acetylcholinesterase From Rat Brain Contains a 20 KDa Hydrophobic Anchor. *Neurochem. Res.* **1994**, *19*, 359−365.
(26) Fernandez, H. L.; Moreno, R. D.; Inestrosa, N. C. Tetrameric (G4) Acetylcholinesterase: Structure, Localization, and Physiological Regulation. *J. Neurochem.* **1996**, *66*, 1335−1346.
(27) Berman, H. A. Interaction of Tetrahydroaminoacridine with Acetylcholinesterase and Butyrylcholinesterase. *Mol. Pharmacol.* **1992**, *41*, 412−418.
(28) Ellman, G. L.; Courtney, K. D.; Andres, V.; Featherstone, J.; Featherstone, R. M. A New and Rapid Colorimetric Determination of Acetylcholinesterase Activity. *Biochem. Pharmacol.* **1961**, *7*, 88−95.
(29) Koh, J. Y.; Choi, D. W. Quantitative Determination of Glutamate Mediated Cortical Neuronal Injury in Cell Culture by Lactate Dehydrogenase Efflux Assay. *J. Neurosci. Methods* **1987**, *20*, 83−90.
(30) Monteith, D. K.; Emmerling, M. R.; Garvin, J.; Theiss, J. C. Cytotoxicity Study of Tacrine, Structurally and Pharmacologically Related Compounds Using Rat Hepatocytes. *Drug Chem. Toxicol.* **1996**, *19*, 71−84.
(31) Galisteo, M.; Rissel, M.; Sergent, O.; Chevanne, M.; Cillard, J.; Guillouzo, A.; Lagadic-Gossmann, D. Hepatotoxicity of Tacrine: Occurrence of Membrane Fluidity Alterations without Involvement of Lipid Peroxidation. *J. Pharmacol. Exp. Ther.* **2000**, *294*, 160−167.
(32) Robey, R. L.; Alt, C. A.; Van Meter, E. E. Reaction of 4-Hydroxy-5-oxymino-3-thiophenecarboxylates with hydrazines. Formation of Pyrazolylthiohydroxamic Acids. *J. Heterocycl. Chem.* **1997**, *34*, 413−428.
(33) Haufel, J.; Breitmaier, E. Synthesis of Pyrazolo Heteroaromatic Compounds by Means of 5-Amino-3-methyl-1-phenylpyrazole-4-carbaldehyde. *Angew. Chem., Int. Ed. Engl.* **1974**, *13*, 604.
(34) Whitaker, J. F. A General Colorimetric Procedure for the Estimation of Enzymes Which Are Linked to the NADH/NAD^+ System. *Clin. Chim. Acta* **1969**, *24*, 23−37.

JM020391N